Front speed enhancement in cellular flows

M. Abel
Institute of Physics, Potsdam University, 14415 Potsdam, Germany
and Dipartimento di Fisica, Università di Roma "La Sapienza," P.zzle Aldo Moro 2, I-00185 Roma, Italy

M. Cencini, D. Vergni, and A. Vulpiani
Dipartimento di Fisica, Università di Roma "La Sapienza," P.zzle Aldo Moro 2, I-00185 Roma, Italy
and Istituto Nazionale Fisica della Materia UdR and SMC Roma "La Sapienza," Roma, Italy

(Received 24 October 2001; accepted 9 January 2002; published 20 May 2002)

The problem of front propagation in a stirred medium is addressed in the case of cellular flows in three different regimes: slow reaction, fast reaction and geometrical optics limit. It is well known that a consequence of stirring is the enhancement of front speed with respect to the nonstirred case. By means of numerical simulations and theoretical arguments we describe the behavior of front speed as a function of the stirring intensity, U. For slow reaction, the front propagates with a speed proportional to $U^{1/4}$, conversely for fast reaction the front speed is proportional to $U^{3/4}$. In the geometrical optics limit, the front speed asymptotically behaves as $U/\ln U$. © *2002 American Institute of Physics.* [DOI: 10.1063/1.1457467]

Front propagation in a stirred medium is an important problem in a number of fields ranging from combustion to plankton dynamics. For a realistic study of such a class of problems one has to take into account the modification of the advecting flow induced by the reaction, e.g., in combustion. However, many features can be understood by neglecting the back-reaction on the velocity field. The problem addressed here is the enhancement of the front speed induced by a certain class of flows. In particular, we consider front propagation in a two dimensional laminar flow with a stationary vortical structure in different regimes, namely slow reaction, fast reaction and geometrical optics limit. This last limit corresponds to a very sharp front propagating as an optical front, i.e., according to the Huygens principle. We provide predictions on the dependence of the front speed on the flow intensity, which are confirmed by numerical simulations.

I. INTRODUCTION

The study of front propagation of a stable phase into an unstable one encompasses several issues of great interest[1] as flame propagation in gases,[2] population dynamics of biological communities (plankton in oceans)[3] and chemical reactions in liquids.[4] A common feature of all these phenomena is that they take place in a strongly deformable medium such as a fluid. The interplay among transport, diffusion and reaction is therefore a crucial problem with several open issues (e.g., for questions concerning combustion, see Ref. 5).

In the most compact model of front propagation the state of the system is described by a single scalar field $\theta(\mathbf{r},t)$, which represents the concentration of products. The field θ vanishes in the regions filled with fresh material (the unstable phase), equals unity where only inert products are left (the stable phase) and takes intermediate values wherever reactants and products coexist, i.e., in the region where production takes place. Here we assume that the concentration of chemicals does not modify the underlying flow. Therefore, in the following, we consider the velocity field as given. This approximation, hardly tenable in the context of flame propagation in gases, is rather appropriate for chemical front propagation in some liquid solutions.[2,5–7] Under these simplifying assumptions, the evolution of θ is described by

$$\partial_t \theta + \mathbf{u}\cdot\nabla\theta = D\Delta\theta + \frac{1}{\tau} f(\theta), \tag{1}$$

where the second term on the lhs accounts for the transport by an incompressible velocity field. On the rhs the first term describes molecular diffusion and the second one describes the production process with time scale τ. We will first consider a production term of Fischer–Kolmogorov–Petrovskii–Piskunov[8] (FKPP) type, i.e., a function $f(\theta)$ convex $[f''(\theta)<0]$ and positive in the interval (0,1), vanishing at its extremes, and $f'(0)=1$. Here we take $f(\theta)=\theta(1-\theta)$. It is also of interest to consider a production term in the form of the Arrhenius law, $f(\theta)=(1-\theta)\cdot\exp(-\theta_c/\theta)$, where θ_c is the activation concentration. The latter choice is more pertinent to the study of flames and/or chemical reactions.[6,7]

Until now we did not specify any details of the velocity field. In many engineering applications $\mathbf{u}$ is turbulent. In this article we investigate front propagation in laminar flows, which, albeit simpler than turbulent ones, show remarkable qualitative similarities with more complex flows.[9] Specifically, we consider a two dimensional stationary incompressible flow with cellular structure (see also Refs. 10–12) $\mathbf{u}=(-\partial_y\psi,\partial_x\psi)$ with the streamfunction[13]

$$\psi(x,y)=\frac{UL}{2\pi}\sin\left(\frac{2\pi x}{L}\right)\sin\left(\frac{2\pi y}{L}\right). \tag{2}$$

We considered L-periodic boundary conditions in y and an infinite extent along the x-axis. This kind of flow is interesting because, in contrast to shear flows, all the streamlines are closed and, therefore, the front propagation is determined by

the mechanisms of contamination of one cell to the other.[10,14] Since we are interested in the propagation in the x-direction, the boundary conditions are set to $\theta(-\infty,y;t)=1$ and $\theta(+\infty,y;t)=0$. The maximum principle ensures that at later times the field still takes values in the range $0\leqslant\theta\leqslant 1$.[1] The instantaneous front speed is defined as

$$v_f(t)=\frac{1}{L}\int_0^L dy\int_{-\infty}^{\infty} dx\,\partial_t\theta(x,y;t). \tag{3}$$

This expression defines the so-called bulk burning rate[11] which coincides with the front speed when the latter exists, but it is also a well defined quantity even when the front itself is not well defined. The asymptotic (average) front speed, v_f, is determined by $v_f=\lim_{T\to\infty}1/T\int dt\, v_f(t)$.

In a medium at rest, it is known that Eq. (1), for FKPP nonlinearity, generates a front propagating, e.g., from left to right with an asymptotic speed $v_0=2\sqrt{D/\tau}$ and a reaction region of thickness $\xi=8\sqrt{D\tau}$.[8] In the more interesting case of a moving medium, the front will propagate with an average speed v_f greater than v_0.[11,12] The front velocity v_f is the result of the interplay among the flow characteristics (i.e., intensity U and length scale L), the diffusivity D and the production time scale τ. The goal of our analysis is to determine the dependence of v_f on such quantities. In particular, introducing the Damköhler number $\mathrm{Da}=L/(U\tau)$ (the ratio of advective to reactive time scales) and the Péclet number $\mathrm{Pe}=UL/D$ (the ratio of diffusive to advective time scales), we seek for an expression of the front speed as an adimensional function $v_f/v_0=\phi(\mathrm{Da},\mathrm{Pe})\geqslant 1$. We will see that a crucial role in determining such a function is played by the renormalization of the diffusion constant and chemical time scale induced by the advection.[14,15]

Moreover, we consider an important limit case, i.e., the so-called geometrical optics limit, which is realized for $(D,\tau)\to 0$ maintaining D/τ constant.[16] In this limit one has a nonzero bare front speed, v_0, while the front thickness ξ goes to zero, i.e., the front is sharp. In this regime the front dynamics is well described by the so-called G-equation[2,6,17]

$$\frac{\partial G}{\partial t}+\mathbf{u}\cdot\boldsymbol{\nabla}G=v_0|\boldsymbol{\nabla}G|. \tag{4}$$

The front is defined by a constant level surface of the scalar function $G(\mathbf{r},t)$. Physically speaking, this limit corresponds to situations in which ξ is very small compared with the other length scales of the problem. Also in this case we provide a simple prediction for the front speed, which turns out to be expressible as an adimensional function $v_f/v_0=\psi(U/v_0)$.

The article is organized as follows. In Sec. II we discuss a theoretical upper bound for the front speed which becomes an equality in the limit of (very) slow reaction. In Sec. III we present a numerical study for slow and fast reaction, comparing the results with a phenomenological model. In Sec. IV we consider the geometrical optics limit. Section V is devoted to some concluding remarks. The Appendix contains the details of the numerical method used in the simulations.

II. UPPER BOUND FOR THE FRONT SPEED

For a generic incompressible flow and a generic production term which has a bounded growth rate, $c(\theta)$, i.e.,

$$c_{\max}=\sup_\theta c(\theta)=\sup_\theta\frac{1}{\tau}\frac{f(\theta)}{\theta}<\infty, \tag{5}$$

it is possible to establish an upper bound for the speed of front propagation. Explicitly, we have

$$v_f\leqslant 2\sqrt{D_{\mathrm{eff}}\,c_{\max}}, \tag{6}$$

where D_{eff} is the effective diffusion coefficient in the x-direction, which can be derived from Eq. (1) by switching off the production term. The key ingredient in deriving the bound (6) is that asymptotically a standard diffusive behavior takes place, which is indeed a generic feature in incompressible fluids.[18] Therefore, in the sequel, we limit our discussion to the asymptotic front propagation properties in flows with standard diffusion. Non-asymptotic properties are surely interesting, as studied in the context of passive transport,[19] but they deserve a specific treatment[20] and are beyond the present aim.

We start the derivation of Eq. (6) by recalling the fundamental relation among the solution of the PDE (1) and the trajectories of particles advected by a velocity field $\mathbf{u}(\mathbf{r},t)$ and subject to molecular diffusion[21,22]

$$\theta(\mathbf{x},t)=\left\langle\theta(\mathbf{r}(0),0)e^{\int_0^t c(\theta(\mathbf{r}(s),s))\,ds}\right\rangle_\eta. \tag{7}$$

The average is performed over the trajectories evolving according to the Langevin equation

$$\frac{d\mathbf{r}(t)}{dt}=\mathbf{u}(\mathbf{r}(t),t)+\sqrt{2D}\,\boldsymbol{\eta}(t) \tag{8}$$

with ending point $\mathbf{r}(t)=\mathbf{x}$. The white noise term $\sqrt{2D}\,\boldsymbol{\eta}(t)$ accounts for molecular diffusion. Since the growth rate is bounded, (7) yields the inequality

$$\theta(t,\mathbf{x})\leqslant\left\langle\theta(\mathbf{r}(0),0)\right\rangle_\eta\exp(c_{\max}t). \tag{9}$$

In the previous inequality, the term in angular brackets denotes the probability that the trajectory ending at $\mathbf{x}$ was initially located at the left of the front interface. For FKPP production term the maximum occurs for $\theta=0$, i.e., $c(\theta)\leqslant c_{\max}=c(0)=1/\tau$. Under very broad conditions, i.e., nonzero molecular diffusivity and finite variance of the velocity vector potential,[18,23,24] it is possible to show that asymptotically the particles undergo a standard diffusion process with an effective diffusion coefficient D_{eff}, always larger than the molecular value D. The issue of single particle diffusion and the problem of finding the effective diffusivity has been the subject matter of a huge amount of work (see, e.g., Ref. 24 for a recent review). In the presence of an asymptotic standard diffusion, we can substitute the term $\langle\theta(\mathbf{r}(0),0)\rangle_\eta$, with the Gaussian result $1-1/2\mathrm{erfc}(-x/\sqrt{2D_{\mathrm{eff}}t})\simeq\exp[-x^2/(4D_{\mathrm{eff}}t)]/\sqrt{2\pi D_{\mathrm{eff}}t}$ with exponential accuracy. We thus obtain $\theta(\mathbf{x},t)\leqslant\exp[c_{\max}t-x^2/(4D_{\mathrm{eff}}t)]/\sqrt{2\pi D_{\mathrm{eff}}t}$. It is thus clear that at the point $\mathbf{x}$ the field θ is exponentially small until a time t of the order of $x/\sqrt{4D_{\mathrm{eff}}c_{\max}}$. We finally obtain the upper bound for the front velocity $v_f\leqslant\sqrt{4D_{\mathrm{eff}}c_{\max}}$, which is Eq. (6).

The bound (6) becomes an equality in the limit of very slow reaction. If τ is the slowest time scale under consideration, advection and molecular diffusion act jointly to build an effective diffusion process, essentially unaffected by the reaction. In this case the front width is large enough and the reaction takes place in a region of effective diffusivity. Therefore, it is allowed to substitute Eq. (1) with an effective reaction-diffusion equation $\partial_t\theta=\Sigma_{i,j}D_{ij}^{\text{eff}}\partial_{ij}^2\theta+(1/\tau)f(\theta)$, where D_{ij}^{eff} is the eddy-diffusivity tensor.[24] For the FKPP nonlinearity, this last equation gives rise to $v_f\simeq 2\sqrt{D_{\text{eff}}/\tau}$, where $D_{\text{eff}}=D_{11}^{\text{eff}}$.[5,10,11] One can find a detailed derivation of this formula in Ref. 14.

For cellular flows, it is known that $D_{\text{eff}}\sim\sqrt{ULD}$.[25–27] Inserting this expression in Eq. (6) one obtains $v_f\propto U^{1/4}$,[10] remarkably close to the observed ones for $Da\ll 1$ (see the next section).

III. FRONT SPEED IN THE REACTION ADVECTION DIFFUSION EQUATION

The bound (6) is very general and holds for generic incompressible flows and production terms. Here, by means of numerical simulations, we consider the front propagation problem arising in the reaction advection diffusion equation (1) for the particular case of the cellular flow (2) of stirring intensity U and FKPP nonlinearity (with characteristic time, τ). In our discussion, we always suppose that the diffusion time scale is the slowest occurring one, i.e., $L^2/D\ll L/U,\tau$ and thus $\text{Pe}\gg 1$ and $\text{Da}\,\text{Pe}\ll 1$.

Now before presenting the numerical results it is helpful to introduce a macroscopic description of the problem which will reduce it to an effective reaction-diffusion process with renormalized coefficients.

The basic observation is that the dynamics of θ in cellular flows is characterized by the cell-size L, so that we can perform a space discretization that reduces each cell, C_i, to a point, i, mapping the domain—a two-dimensional infinite strip—onto a one-dimensional lattice. The field θ becomes a function defined on the lattice $\Theta_i=L^{-2}\int_{C_i}\theta\,dx\,dy$. Integrating Eq. (1) over the cell C_i, we obtain $\dot{\Theta}_i=J_{i+1}-J_i+\chi_i$ where $J_i=L^{-2}\int_{\text{left}}D\partial_x\theta\,dy$ is the flux of matter through the left boundary of the ith cell, and $\chi_i=L^{-2}\int_{C_i}\tau^{-1}f(\theta)dx\,dy$ is the rate of change of Θ_i due to reaction taking place within the cell. On the basis of the numerical results (see below), we will show that the space-discretized macroscopic reaction-diffusion equation

$$\frac{d}{dt}\Theta_i=D_{\text{eff}}\left(\frac{1}{2}\Theta_{i+1}-\Theta_i+\frac{1}{2}\Theta_{i-1}\right)+\frac{1}{\tau_{\text{eff}}}F(\Theta_i) \qquad (10)$$

is a pretty good model for the front dynamics. The effect of the advective field is to *renormalize* the values of the diffusivity, $D\to D_{\text{eff}}(D,U,L)$, and the reaction time scale, $\tau\to\tau_{\text{eff}}(\tau,U,L)$. This is why the velocity does not appear any more in the effective dynamics, described by Eq. (10).[10,14] The renormalized diffusivity D_{eff} accounts for the process of diffusion from cell to cell as a result of the nontrivial interaction of advection and molecular diffusion.[25–27] The renormalized reaction time τ_{eff} amounts to the time that it takes for a single cell to be filled by inert material, and depends on the interaction of advection and production. Of course, also the production term will be affected, i.e., $f\to F$, but, as we will see, such a modification is not dramatic. Indeed, the modified production term turns always to be in the FKPP universality class.

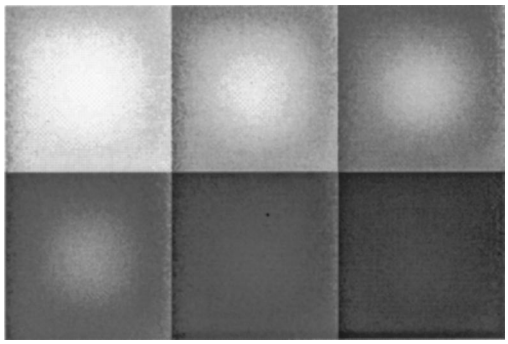

FIG. 1. Six snapshots of the field θ within the same cell, at six successive times with a delay $\tau/6$ (from left to right, top to bottom), as a result of the numerical integration of Eq. (1). Here $\text{Da}\simeq 0.4$, $\text{Pe}\simeq 315$. Black stands for $\theta=1$, white for $\theta=0$.

The limiting speed of the front in the moving medium turns out to be $v_{\text{eff}}\sim\sqrt{D_{\text{eff}}/\tau_{\text{eff}}}$, similar to Eq. (6).[14] The problem is now reduced to derive the expressions for the renormalized parameters by means of physical considerations.

It is worthwhile to remark that model (10) has just a phenomenological origin (see Refs. 10 and 19) supported by numerical evidences.

In the following sections, using as an interpretative framework the above described macroscopic model, we will present the results of detailed numerical simulations for slow ($\text{Da}\ll 1$) and fast ($\text{Da}\gg 1$) reaction.

A. Slow reaction regime

At small Da, the reaction is significantly slower than the advection, and consequently the region where the reaction takes place extends over several cells, i.e., the front is distributed. To obtain the expression of D_{eff} we neglect the reaction term in Eq. (1), which reduces to the equation for a passive scalar in a cellular flow. This is a well studied problem, the solution of which is[25–27]

$$\frac{D_{\text{eff}}}{D}\sim\text{Pe}^{1/2},\quad \text{Pe}\gg 1. \qquad (11)$$

For large Pe (D small) the cell-to-cell diffusion mechanism can be qualitatively understood in the following way. The probability, p, for a particle to jump across the boundary of the cell, within a circulation time L/U, by virtue of molecular diffusion can be estimated as the ratio of the diffusive motion across streamlines, $O(\sqrt{DL/U})$, to advective motion along streamlines, $O(L)$. As a result $p\sim(D/(UL))^{1/2}$, hence the effective diffusivity $D_{\text{eff}}\sim pUL\sim D\text{Pe}^{1/2}$.

To obtain the expression of the typical time it takes for a whole cell to react, let us concentrate on the reaction in a single cell: it is first invaded by a mixture of reactants and products (with a low content of products, $\Theta_i\ll 1$) on the fast advective time scale; subsequently complete reaction ($\Theta_i\approx 1$) is achieved on the slower time scale $\tau_{\text{eff}}\simeq\tau$ (see Fig. 1).

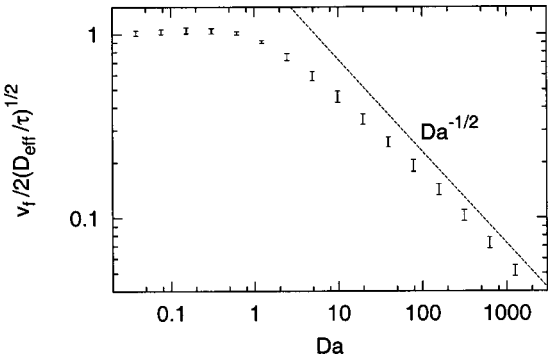

FIG. 2. The ratio of measured front speed, v_{eff}, to the maximal one, $\sqrt{4D_{\mathrm{eff}}/\tau}$, as a function of the Damköhler number, Da. For $\mathrm{Da}\ll 1$ the front propagates with the maximal velocity whereas for $\mathrm{Da}\gg 1$ the speed slows down with increasing Da. The straight line $\mathrm{Da}^{-1/2}$ is drawn for reference. Note that there are two contributions to the error bars: from the uncertainty on the v_{eff} and that one on the effective diffusion coefficient D_{eff}.

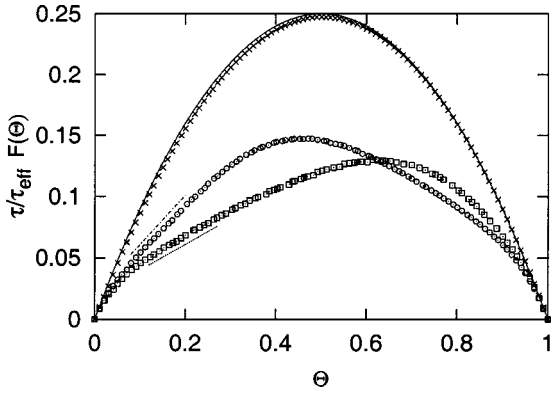

FIG. 4. The renormalized reaction term $\tau/\tau_{\mathrm{eff}}F(\Theta)$ for three different parameter: $\mathrm{Da}\simeq 4$ (□), $\mathrm{Da}\simeq 2$ (○) and $\mathrm{Da}\simeq 0.4$ (×). The continuous line shows $f(\theta)$. The dotted and dash-dotted lines are the slopes (0.2 and 0.4) proportional to Da^{-1} in the region of slow advection.

In this regime, the front speed is well approximated by the homogenization result $v_{\mathrm{f}}=2\sqrt{D_{\mathrm{eff}}}$, discussed in the previous section. To check these ideas, we performed numerical simulations of Eq. (1), with a FKPP production term (see the Appendix for details on the numerical technique). In Fig. 2, we show the result of the calculations for the front speed v_{f} in dependence on Da; the slow reaction corresponds to the plateau at $\mathrm{Da}\ll 1$.

B. Fast reaction regime

We now have to repeat the estimation of D_{eff} and τ_{eff} for the fast reaction regime, i.e., for large Da. Since we work always in the regime of large Peclet numbers, all the above arguments for the effective diffusion still hold, while the effective time scale is different. At large Da, the ratio of time scales reverses, and in a (now short) time τ two sharply separated phases emerge inside the cell. In this regime indeed, the interface is thin compared to the cell size. The cell filling process is characterized by an inward spiral motion of the outer, stable phase (see Fig. 3), at a speed proportional to U, as it usually happens for a front in a shear flow at large Da. Therefore, the $\theta=1$ phase fills the whole cell on the advective time scale, giving $\tau_{\mathrm{eff}}\simeq L/U$. With respect to the upper bound (6) we observe for fast reaction a significative slowing down of the front speed signaled by a different scaling dependence on the parameters U, D, L, τ (see Fig. 2). We now have to look at the shape of the effective reaction term $\tau_{\mathrm{eff}}^{-1}F(\Theta)$ appearing in the renormalized equation (10). As shown in Fig. 4, for small Da, the effective production term is indistinguishable from the "bare" one. Increasing Da, the reaction rate tends to reduce, inducing the slowing down of the front speed. For $\Theta\approx 0$, the effective production term essentially coincides with the microscopic one. However, there is an intermediate regime characterized by a linear dependence on the cell-averaged concentration, with a slope proportional to Da^{-1}. This is in agreement with a typical effective reaction time $\tau_{\mathrm{eff}}\sim\tau\mathrm{Da}$ [see below Eq. (12)]. To measure the macroscopic quantities $F(\Theta)$ and Θ, one simply integrates numerically both θ and $f(\theta)$ at a fixed time over a cell volume.

It is worthwhile to remark that, notwithstanding the change of shape of the effective chemical potential, the production term remains in the FKPP universality class.

Let us stress that what we call fast reaction regime is still not in the geometrical optics limit. Indeed, to obtain this limit it is not sufficient to take τ small, but one has to take also D small in such a way that $v_0\sim 2\sqrt{D/\tau}$ is constant when (D,τ) goes to zero and the front thickness $\xi\propto\sqrt{D\tau}$ is negligible with respect to the cell size. In the fast reaction regime studied here the condition on the front thickness holds.

Collecting the information about fast and slow reaction,

$$\frac{\tau_{\mathrm{eff}}}{\tau}\sim\begin{cases}1 & \mathrm{Da}\ll 1,\\ \mathrm{Da}, & \mathrm{Da}\gg 1,\end{cases} \tag{12}$$

and $D_{\mathrm{eff}}\sim D\mathrm{Pe}^{1/2}$, we can derive the scaling of the effective speed of front propagation for a cellular flow. Indeed, recalling that $v_{\mathrm{f}}\sim\sqrt{D_{\mathrm{eff}}/\tau_{\mathrm{eff}}}$, we have the final result

$$\frac{v_{\mathrm{f}}}{v_0}\sim\begin{cases}\mathrm{Pe}^{1/4}, & \mathrm{Da}\ll 1,\mathrm{Pe}\gg 1,\\ \mathrm{Pe}^{1/4}\mathrm{Da}^{-1/2}, & \mathrm{Da}\gg 1,\mathrm{Pe}\gg 1.\end{cases} \tag{13}$$

The case of $\mathrm{Pe}\ll 1$ is less interesting because the dynamics is dominated by diffusion.

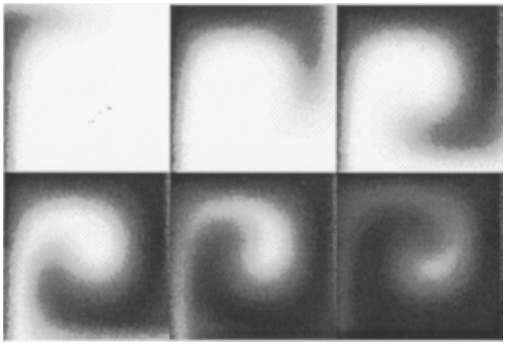

FIG. 3. Six snapshots of the field θ within the same cell, at six successive times with a delay $(L/U)/6$ (left to right, top to bottom). Here $\mathrm{Da}=4$, $\mathrm{Pe}=315$. A spiral wave invades the interior of the cell, with a speed comparable to U.

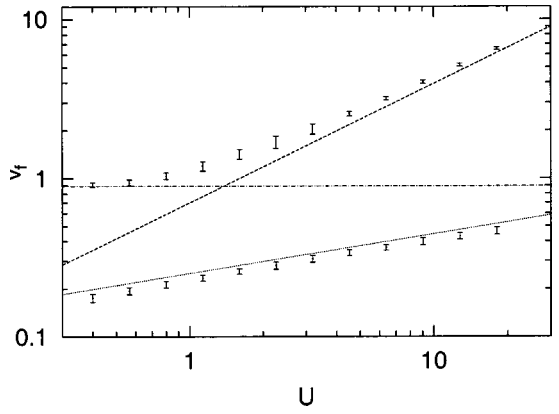

FIG. 5. The front speed v_f as a function of U, the typical flow velocity. The lower curve shows data at $\tau=20.0$ (fast advection). The upper curve shows data at $\tau=0.2$ (slow advection). For comparison, the scalings $U^{1/4}$ and $U^{3/4}$ are shown as dotted and dashed lines, respectively. The horizontal line indicates v_0, the front velocity without advection, for $\tau=0.2$.

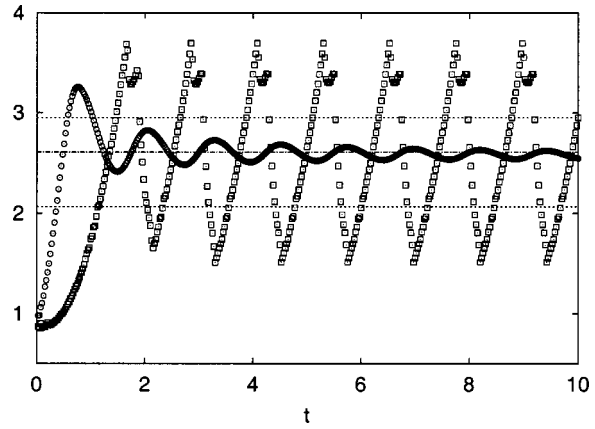

FIG. 6. Front velocity as a function of time, $v_f(t)$ measured in the standard way (3) (□), and as $x_M(t)/t$ (○). The straight lines represents the average (over a period) of the measured value, and the lower and upper bounds. The simulation parameters are $U=4$, $v_0=1$ and $L=2\pi$.

At small Da the front propagates with an effective velocity scaling as the upper bound derived above, that is, as $\mathrm{Pe}^{1/4}$. At large Da, the front speed enhanced is less effective than at small Da: according to Eq. (13), we have $v_f/v_0 \sim \mathrm{Da}^{-1/2}$ for $\mathrm{Da}\gg 1$. In terms of the typical velocity of the cellular flow, we have $v_f \propto U^{1/4}$ for slow reaction ($U\gg L/\tau$, or equivalently $\mathrm{Da}\ll 1$) whereas $v_f \propto U^{3/4}$ for fast reaction ($U \ll L/\tau$, or $\mathrm{Da}\gg 1$). The scaling $v_f \propto U^{1/4}$ for slow reaction (i.e., fast advection) is a consequence of the well known result $D_{\mathrm{eff}} \propto D\mathrm{Pe}^{1/2}$ (Ref. 25) in the homogenization limit;[11,14] it has been obtained in Ref. 10. The numerical results are summarized in Fig. 5.

As a remark we mention that, for the class of boundary conditions investigated here, where the region of initially burnt material extends to infinity, no quenching[28] takes place no matter the used production term. Indeed, Arrhenius-type nonlinearity substantially gives the same results as those of FKPP-type reaction presented above, i.e., one has the two scaling laws $v_f \propto U^{1/4}$ and $v_f \propto U^{3/4}$ at fast and slow advection, respectively (see Ref. 14).

IV. FRONT SPEED IN THE GEOMETRICAL OPTICS REGIME

When the front thickness and the reaction time are much smaller than the length and time scales of the velocity field fluctuations one has the geometrical optics regime.[16,29] In this case the front is a sharp interface separating the reactants from the products, and can be modeled in the framework of the G-equation (4).[6,16] Physically speaking, one uses the G-equation when the front thickness is very thin and it is hard to resolve the diffusive scale.

As far as the cellular flow is concerned, the front border is wrinkled by the velocity field during propagation and its length increases until pockets of fresh material develop.[30–32] After this, the front propagates periodically in space and time with an average speed v_f, which is enhanced with respect to the propagation speed v_0 of the fluid at rest[33] (see Ref. 31 for some pictorial views).

The problem addressed here is the dependence of the effective speed v_f on the flow intensity, U, and the bare velocity, v_0, that is expected of the form[6]

$$\frac{v_f}{v_0} = \psi\left(\frac{U}{v_0}\right), \tag{14}$$

where $\psi(\mathcal{U})$ is a function which depends on the flow details.

As far as we know, apart from very simple shear flows (for which $\psi(\mathcal{U})=1+\mathcal{U}$),[10,16] there are no methods to compute $\psi(\mathcal{U})$ from first principles. Mainly one has to resort to numerical simulations and phenomenological arguments.

For turbulent flows, by means of dynamical renormalization group techniques, Yakhot[34] proposed

$$\frac{v_f}{v_0} = e^{d(U/v_f)^\alpha}, \tag{15}$$

where $d=1$ and $\alpha=2$. Now U indicates the root mean squared average velocity (see also Refs. 6 and 35). Therefore, from (15) one has that $v_f \to U/\sqrt{\ln(U)}$ for $U\to\infty$.

For the cellular flow under investigation, albeit the exact form of the function $\psi(\mathcal{U})$ is not known, a simple argument can be given for an upper and a lower bound by mapping the front dynamics onto a one-dimensional problem. The starting point is the following observation. In the optical regime, since the interface is sharp, i.e., $\theta(x,y)$ is a two-valued function ($\theta=1$ and $\theta=0$), we can track the farther edge of the interface between product and material $(x_M(t),y_M(t))$, which is defined as the rightmost point (in the x-direction) for which $\theta(x_M,y_M;t)=1$. Then we can define a velocity

$$\tilde{v}_f = \lim_{t\to\infty} \frac{x_M(t)}{t}, \tag{16}$$

which gives an equivalent value of the standard definition within less than 2% (see Fig. 6). In Fig. 7 we show the time evolution of the point $(x_M(t),y_M(t))$. After a transient, in the unit cell $[0,2\pi]$ (we describe the case $L=2\pi$, i.e., the one adopted here) the point $(x_M(t),y_M(t))$ moves to the right along the separatrices of the streamfunction (2), so that

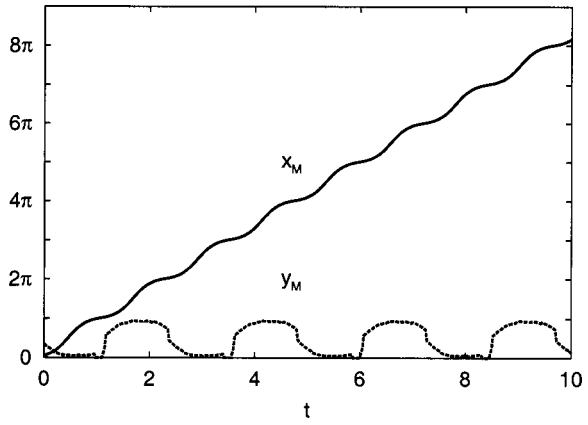

FIG. 7. Time evolution of the edge point: $x_M(t)$ (solid line) and $y_M(t)$ (dashed line). The simulation parameters are the ones of Fig. 6.

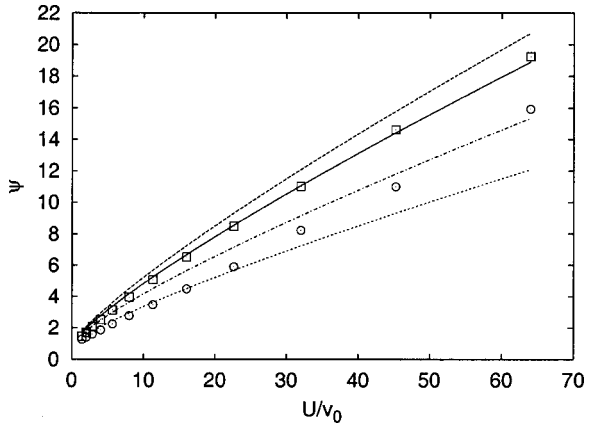

FIG. 8. The measured $\psi(U/v_0)$ as a function of U/v_0 (□), the Yakhot formula (15) with $\alpha=2$ (○) and $d=1/\sqrt{2}$, the function ψ_β for $\beta=1,\frac{1}{2}$ (dashed and dotted lines) and for $\beta=0.89$ (solid line). The dashed-dotted line is the bound (19).

$y_M(t)$ is essentially close to the values 0 or π. Along this path one can reduce the edge dynamics to the $1d$-problem

$$\frac{dx_M}{dt}=v_0+U\beta|\sin(x_M(t))|, \tag{17}$$

where the second term of the rhs is the horizontal component of the velocity field. We have neglected the y-dependence, replacing it with a constant β which takes into account the average effect of the vertical component of the velocity field along the path followed by (x_M,y_M). By solving (17) in the interval $x_M\in(0,2\pi)$ one obtains the time, T, needed for x_M to reach the end of the cell. The front speed, as the speed of the edge particle, is then given by $v_f=2\pi/T$. The final result is

$$\psi_\beta(\mathcal{U})=\pi\sqrt{(\mathcal{U}\beta)^2-1}\,\ln^{-1}\left(\frac{\mathcal{U}+\sqrt{(\mathcal{U}\beta)^2-1}}{\mathcal{U}-\sqrt{(\mathcal{U}\beta)^2-1}}\right). \tag{18}$$

Note that (18) is valid only for $\mathcal{U}\beta\geqslant 1$. We have taken $\beta=1$ for the upper bound and $\beta=\frac{1}{2}$ [which is the average of $|\cos(y)|$ between 0 and π] for the lower bound. We have also computed the average of $|\cos(y_M(t))|$ in a period of its evolution (see Fig. 7), obtaining $\beta\approx 0.89$ which gives indeed a very good approximation of the measured curve (see Fig. 8). We stress that the theoretical curve is not a fit, but it just involves the measured parameter β.

This agreement is an indication that the average of $|\cos(y_M(t))|$ depends on U and v_0 very weakly (as we checked numerically). Previous studies[32] reported an essentially linear dependence of the front speed on the flow intensity, i.e., $v_f\propto U$ for large U which is not too far but different from our result. A rigorous bound has been obtained in Ref. 36 by using the G-equation:

$$v_f\geqslant U/(\log(1+U/v_0)). \tag{19}$$

As one can see from Fig. 8, the lower bound (19) seems to be closer to the numerical data than the one obtained with $\beta=\frac{1}{2}$ in (18). From Eq. (18), asymptotically (i.e., for $U\gg v_0$) one has $v_f\sim U/\ln(U)$ which corresponds to (15) for $\alpha=1$. Expressions as (15) have been proposed for flows with many scales as, e.g., turbulent flows, and in the literature different values of α have been reported.[6,37] The fact that also the simple one-scale vortical flow investigated here displays such a behavior may be incidental. However, we believe that it can be due to physical reasons. Indeed, the large scale features of the flow, e.g., the absence of open channels (like for the shear flow), can be more important than the detailed multi-scale properties of the flow.[38]

A definite answer to this question is beyond the scope of this article, however it could be an interesting point for future investigations.

V. CONCLUSIONS

We addressed the problem of front speed enhancement induced by stirring due to a cellular flow in different regimes. In the slow reaction case a rather general result (based on homogenization techniques) gives $v_f\sim U^{1/4}$; for the fast reaction case, physical arguments give $v_f\sim U^{3/4}$. In the geometrical optics limit one finds that v_f is a linear function of U, apart from logarithmic corrections. All these results has been confirmed by numerical simulations.

The steady cellular flow treated here, albeit its simplicity, provides a paradigm that can be insightful for the study of front propagation in more general flows. For instance, in the geometrical optics limit the asymptotical behavior $v_f\sim U/\ln(U)$ is rather similar to the one found by Yakhot ($v_f\sim U/\sqrt{\ln(U)}$) (Ref. 34) for turbulent velocity fields.

One could conjecture that there are nontrivial reasons for this similarity: the front propagation principally involves the largest scales. In this context, it is not surprising that a multiscale process (as turbulence) or a single scale process can yield similar results.

ACKNOWLEDGMENTS

We gratefully thank A. Celani and A. Torcini, who recently collaborated with us on the issue here discussed. We also acknowledge stimulating discussions with R. M. McLaughlin and M. Vergassola. This work has been partially supported by the INFM *Parallel Computing Initiative* and MURST (Cofinanziamento *Fisica Statistica e Teoria della Materia Condensata*). M.A. has been partially supported by

the European Network *Intermittency in Turbulent Systems* (FMRX-CT98-0175). M.C., D.V. and A.V. acknowledge support from the INFM *Center for Statistical Mechanics and Complexity* (SMC).

APPENDIX: NUMERICAL METHOD

We introduce a lattice of mesh size Δx and Δy (for the sake of simplicity we assume $\Delta x=\Delta y$) so that the scalar field is defined on the points $\mathbf{x}_{n,m}=(n\Delta x, m\Delta y)$: $\theta_{n,m}(t)=\theta(n\Delta x, m\Delta y, t)$.

Giving the field at time t, the algorithm computes the field at time $t+\Delta t$, and the integration method depends on which kind of physical regime we are interest in: reaction-advection-diffusion equation (1) or optical limit (4).

1. Reaction diffusion equation

In numerical approaches one is forced to discretize the dynamics, so let us consider the case of a velocity field which is always zero apart from δ-impulses at times $t=0$, $\pm\Delta t, \pm 2\Delta t, \pm 3\Delta t, \ldots$:

$$\mathbf{u}(\mathbf{x},t)=\sum_{n=-\infty}^{\infty}\mathbf{u}(\mathbf{x})\,\delta(t-n\Delta t). \tag{A1}$$

In such a case the Lagrangian evolution is given by a conservative map (in 2D the map is symplectic due to incompressibility)

$$\mathbf{x}(t+\Delta t)=\mathbf{F}^{\Delta t}(\mathbf{x}(t)). \tag{A2}$$

If also the production term is zero apart from δ-impulses,

$$f(\theta)=\sum_{n=-\infty}^{\infty} g(\theta)\,\delta(t-n\Delta t), \tag{A3}$$

one can introduce a reaction map

$$\theta(t+\Delta t)=G_{\Delta t}(\theta(t)). \tag{A4}$$

Let us remark that choosing a δ-impulsed production term can be particularly relevant in some experimental settings, i.e., when one considers periodic illumination in light-sensitive chemical reactions as in Ref. 39. The concentration field $\theta(\mathbf{x},t+\Delta t-0)$ is obtained from $\theta(\mathbf{x},t+0)=G_{\Delta t}(\theta(\mathbf{x},t))$ solving the bare diffusion equation $\partial_t\theta=D\nabla^2\theta$:

$$\theta(\mathbf{x},t+\Delta t-0)=\frac{1}{(2\pi)^{d/2}}\int e^{-\eta^2/2}\theta(\mathbf{x}-\sqrt{2D\Delta t}\,\boldsymbol{\eta},t+0)\,\mathrm{d}\boldsymbol{\eta}, \tag{A5}$$

or, in other terms,

$$\theta(\mathbf{x},t+\Delta t)=\langle G_{\Delta t}(\theta(\mathbf{F}^{-\Delta t}(\mathbf{x}-\sqrt{2D\Delta t}\,\boldsymbol{\eta}(t)),t))\rangle_{\eta}, \tag{A6}$$

which is equivalent to Eq. (7). Let us remark that Eq. (A6) is exact if both the velocity field and the reaction are δ-impulsed processes. However, one can also use the formula (A6) as a practical method for the numerical integration of Eq. (1) if one assumes small enough Δt, so that the Lagrangian and reaction maps are given at the lowest order by

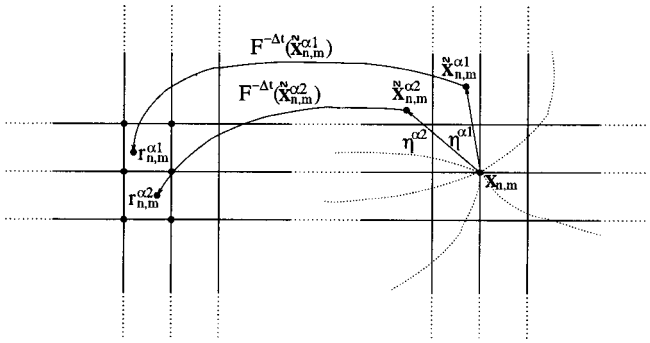

FIG. 9. Pictorial scheme of the numerical algorithm for RAD systems. Here $\boldsymbol{\eta}^{\alpha}=\sqrt{2D\,\Delta t}\,\mathbf{W}^{\alpha}$ where $\mathbf{W}^{\alpha}$ is a standard Gaussian variable.

$$\mathbf{F}^{\Delta t}(\mathbf{x})\simeq\mathbf{x}+\mathbf{u}(\mathbf{x})\Delta t, \quad G_{\Delta t}\simeq\theta+\frac{\Delta t}{\tau_r}f(\theta).$$

From an algorithmic point of view the whole process between t and $t+\Delta t$, Eq. (A6), can be divided into three steps: (1) diffusive, (2) advective, and (3) reactive. The first two steps determine the origin of the Lagrangian trajectory evolving with a given noise realization $\boldsymbol{\eta}$ and ending in $\mathbf{x}$. In the third step, the reaction at point $\mathbf{x}$ for the advected/diffused passive scalar θ is computed:

(1) backward diffusion: $\mathbf{x}\to\mathbf{x}-\sqrt{2D\Delta t}\,\boldsymbol{\eta}$,
(2) backward advection by the Lagrangian map:
$\mathbf{x}-\sqrt{2D\Delta t}\,\boldsymbol{\eta}\to\mathbf{F}^{-\Delta t}(\mathbf{x}-\sqrt{2D\Delta t}\,\boldsymbol{\eta})$,
(3) forward reaction:
$\theta(t+\Delta t)=G_{\Delta t}(\theta(t))$.

These three steps can be numerically implemented as follows. For each grid point $\mathbf{x}_{n,m}$, one uses N independent Gaussian processes $\mathbf{W}^{\alpha}$, $\alpha=1,\ldots,N$, $N\gg 1$, and computes $\tilde{\mathbf{x}}^{\alpha}_{n,m}=\mathbf{x}_{n,m}-\sqrt{2D\,\Delta t}\,\mathbf{W}^{\alpha}$. Then, using the Lagrangian backward propagator, $\mathbf{r}^{\alpha}_{n,m}=\mathbf{F}^{-\Delta t}(\tilde{\mathbf{x}}^{\alpha}_{n,m})$. For $\theta_{n,m}(t+\Delta t)$ one needs the values of θ at time t in the positions $\mathbf{r}^{\alpha}_{n,m}$. Typically the $\mathbf{r}^{\alpha}_{n,m}$ are not on the grid points $(n\Delta x, m\Delta y)$; nevertheless, we can compute the value $\theta(\mathbf{r}^{\alpha}_{n,m},t)$ using simple linear interpolation from $\theta_{n,m}(t)$. Therefore, we have

$$\theta_{n,m}(t+\Delta t)=\frac{1}{N}\sum_{\alpha=1}^{N}G[\,\theta(\mathbf{r}^{\alpha}_{n,m},t)\,].$$

To correctly simulate the diffusion process we have to impose a relation between D, Δx and Δt to assure that diffusion transports a particle over distances $\sim\sqrt{2D\,\Delta t}$ much larger than the grid size Δx (see Fig. 9).

2. Geometrical optics limit

Similar to the previous case, one can integrate the dynamics of the optical front using a two step discrete-time process. Starting from the field $\theta_{n,m}$ at time t, one can obtain the field at time $t+\Delta t$ with the following algorithm:

(1) Using the Lagrangian propagator one evolves the interface between burned and unburned region.

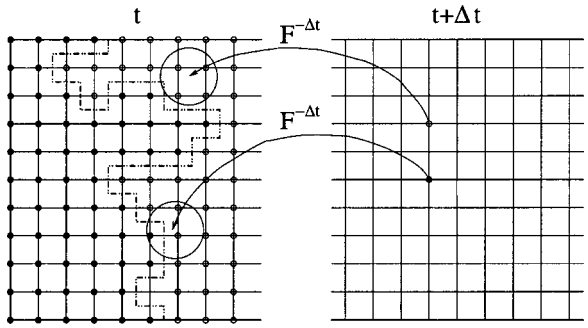

FIG. 10. Pictorial scheme of the numerical algorithm for the geometrical optics limit.

(2) At each point of the evolved interface one constructs a circle of radius $v_0\,\Delta t$, burning the points within the circles.

To numerically implement such an algorithm one can proceed as follows: starting in a grid point, $\mathbf{x}_{n,m}$, of the scalar field at time $t+\Delta t$ one applies the backward evolution arriving at the point $\mathbf{y}=\mathbf{F}^{-\Delta t}\mathbf{x}_{n,m}$ at the time t. On this point we construct the circle of radius $v_0\,\Delta t$. If in this circle there is at least one burned point of the scalar field at time t, we fix $\theta(\mathbf{x}_{n,m};t+\Delta t)=1$, otherwise $\theta(\mathbf{x}_{n,m};t+\Delta t)=0$, see Fig. 10.

Also in this case we have to care that the radius of circle $v_0\,\Delta t$ has to be much larger than the grid size Δx.

[1] J. Xin, ''Front propagation in heterogeneous media,'' SIAM Rev. **42**, 161 (2000).
[2] F. A. Williams, *Combustion Theory* (Benjamin-Cummings, Menlo Park, 1985).
[3] E. R. Abraham, ''The generation of plankton patchiness by turbulent stirring,'' Nature (London) **391**, 577 (1998); E. R. Abraham, C. S. Law, P. W. Boyd, S. J. Lavender, M. T. Maldonado, and A. R. Bowie, ''Importance of stirring in the development of an iron-fertilized phytoplankton bloom,'' *ibid.* **407**, 727 (2000).
[4] J. Ross, S. C. Müller, and C. Vidal, ''Chemical waves,'' Science **240**, 460 (1988); I. R. Epstein, ''The consequences of imperfect mixing in autocatalytic chemical and biological systems,'' Nature (London) **374**, 231 (1995).
[5] P. D. Ronney, ''Some open issues in premixed turbulent combustion,'' in *Modeling in Combustion Science*, edited by J. Buckmaster and T. Takeno, Springer-Verlag Lecture Notes in Physics (Springer, New York, 1994), pp. 3–22.
[6] N. Peters, *Turbulent Combustion* (Cambridge University Press, Cambridge, 2000).
[7] P. D. Ronney, B. D. Haslam, and N. O. Rhys, ''Front propagation rates in randomly stirred media,'' Phys. Rev. Lett. **74**, 3804 (1995).
[8] A. N. Kolmogorov, I. G. Petrovskii, and N. S. Piskunov, ''Study of the diffusion equation with growth of the quantity of matter and its application to a biology problem,'' Moscow Univ. Bull. Math. **1**, 1 (1937); R. A. Fischer, ''The wave of advance of advantageous genes,'' Ann. Eugenics **7**, 355 (1937).
[9] J. M. Ottino, *The Kinematics of Mixing: Stretching, Chaos and Transport* (Cambridge University Press, Cambridge, 1989); A. Crisanti, M. Falcioni, G. Paladin, and A. Vulpiani, ''Lagrangian chaos: Transport, mixing and diffusion in fluids,'' Riv. Nuovo Cimento **14**, 1 (1991).
[10] B. Audoly, H. Beresytcki, and Y. Pomeau, ''Réaction diffusion en écoulement stationnaire rapide,'' C. R. Acad. Sci., Ser. IIb: Mec., Phys., Chim., Astron. **328**, 255 (2000).
[11] P. Constantin, A. Kiselev, A. Oberman, and L. Ryzhik, ''Bulk burning rate in passive-reactive diffusion,'' Arch. Ration. Mech. Anal. **154**, 53 (2000).
[12] A. Kiselev and L. Ryzhik, ''Enhancement of the traveling front speeds in reaction-diffusion equations with advection,'' Ann. I.H. Poincaré **18**, 309 (2001).
[13] T. H. Solomon and J. P. Gollub, ''Chaotic particle transport in time-dependent Rayleigh–Bénard convection,'' Phys. Rev. A **38**, 6280 (1988); ''Passive transport in steady Raleigh–Bénard convection,'' Phys. Fluids **31**, 1372 (1988).
[14] M. Abel, A. Celani, D. Vergni, and A. Vulpiani, ''Front propagation in laminar flows,'' Phys. Rev. E **64**, 046307 (2001).
[15] A. C. Marti, F. Sagues, and J. M. Sancho, ''Front dynamics in turbulent media,'' Phys. Fluids **9**, 3851 (1997); ''Reaction-diffusion fronts under stochastic advection,'' Phys. Rev. E **56**, 1729 (1997).
[16] P. F. Embid, A. J. Majda, and P. E. Souganidis, ''Comparison of turbulent flame speeds from complete averaging and the G-equation,'' Phys. Fluids **7**, 2052 (1995).
[17] A. R. Kerstein, W. T. Ashurst, and F. A. Williams, ''Field equation for interface propagation in an unsteady homogeneous flow field,'' Phys. Rev. A **37**, 2728 (1988).
[18] M. Avellaneda and A. Majda, ''Stieltjes integral representation and effective diffusivity bounds for turbulent transport,'' Phys. Rev. Lett. **62**, 753 (1989); M. Avellaneda and M. Vergassola, ''Stieltjes integral representation of effective diffusivities in time-dependent flows,'' Phys. Rev. E **52**, 3249 (1995).
[19] W. Young, A. Pumir, and Y. Pomeau, ''Anomalous diffusion of tracer in convection rolls,'' Phys. Fluids A **1**, 462 (1989).
[20] G. Boffetta, A. Celani, M. Cencini, G. Lacorata, and A. Vulpiani, ''Non-asymptotic properties of transport and mixing,'' Chaos **10**, 50 (2000).
[21] M. Freidlin, *Markov Processes and Differential Equations* (Birkhauser, Boston, 1996).
[22] S. Fedotov, ''Scaling and renormalization for the Kolmogorov–Petrovskii–Piskunov equation with turbulent convection,'' Phys. Rev. E **55**, 2750 (1997).
[23] R. H. Kraichnan, ''Turbulent diffusion: evaluation of primitive and renormalized perturbation series by Padé approximations and by expansion of Stieltjes transforms into contributions from continuous orthogonal function,'' in *The Padé Approximants in Theoretical Physics* (Academic, New York, 1970), p. 129.
[24] A. J. Majda and P. R. Kramer, ''Simplified models for turbulent diffusion: Theory, numerical modeling and physical phenomena,'' Phys. Rep. **314**, 237 (1999).
[25] Y. Pomeau, ''Dispersion dans un écoulement en présence de zones de recirculation,'' C. R. Acad. Sci. **301**, 1323 (1985).
[26] B. I. Shraiman, ''Diffusive transport in Rayleigh–Bénard convection cell,'' Phys. Rev. A **36**, 261 (1987).
[27] M. N. Rosenbluth, A. L. Berk, I. Doxas, and W. Horton, ''Effective diffusion in laminar convective flows,'' Phys. Fluids **30**, 2636 (1987).
[28] P. Constantin, A. Kiselev, and L. Ryzhik, ''Quenching of flames by fluid advection,'' Commun. Pure Appl. Math. **54**, 1320 (2001).
[29] R. M. McLaughlin and J. Zhu, ''The effect of finite front thickness on the enhanced speed of propagation,'' Combust. Sci. Technol. **129**, 89 (1997).
[30] W. T. Ashurst and G. I. Shivanshinsky, ''On flame propagation through periodic flow fields,'' Combust. Sci. Technol. **80**, 159 (1991).
[31] R. C. Aldredge, ''The scalar-field front propagation equation and its applications,'' in *Modeling in Combustion Science*, edited by J. Buckmaster and T. Takeno, Springer-Verlag Lecture Notes in Physics (Springer, New York, 1994), pp. 23–35.
[32] R. C. Aldredge, ''Premixed flame propagation in a high-intensity, large-scale vortical flow,'' Condens. Matter Phys. **106**, 29 (1996).
[33] M. Cencini, A. Torcini, D. Vergni, and A. Vulpiani, ''Thin front propagation in steady and unsteady cellular flows'' (LANL e-print archive nlin/0201015).
[34] V. Yakhot, ''Propagation velocity of premixed turbulent flame,'' Combust. Sci. Technol. **60**, 191 (1988).
[35] M. Chertkov and V. Yakhot, ''Propagation of a Huygens front through turbulent medium,'' Phys. Rev. Lett. **80**, 2837 (1998).
[36] A. Oberman, Ph.D. thesis, University of Chicago, 2001.
[37] A. R. Kerstein and W. T. Ashurst, ''Propagating rate of growing interfaces in stirred fluids,'' Phys. Rev. Lett. **68**, 934 (1992).
[38] W. T. Ashurst, ''Flame propagation through swirling eddies, a recursive pattern,'' Combust. Sci. Technol. **92**, 87 (1993).
[39] V. Petrov, Q. Ouyang, and H. L. Swinney, ''Resonant pattern formation in a chemical system,'' Nature (London) **388**, 655 (1997); M. Dolnik, A. M. Zhabotinsky, and I. R. Epstein, ''Resonant suppression of Turing patterns by periodic illumination,'' Phys. Rev. E **63**, 026101 (2001).